



Effect of binning on measurements of the transverse momentum distribution of Z/γ^* bosons in proton-proton collisions

Thi Kieu Oanh Doan

kieu_y5@yahoo.com

Tay Bac University, Son La, Vietnam

Thi Hong Van Nguyen

nhvan@iop.vast.vn

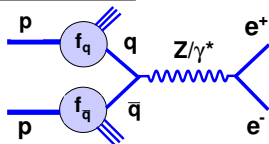
Institute of Physics, Ha Noi, Vietnam

- Transverse momentum of Z/γ^* (p_T^Z)
- Latest p_T^Z measurements at the LHC
- Why binning effect?
- What we do in binning effect study?
 1. The “true” p_T^Z spectrum
 2. Resolution of p_T^Z measurements
 3. Purity, binning and smearing
 4. Unfolding the reconstructed p_T^Z spectra
- Results
- Conclusion

Transverse momentum of Z/γ^* (p_T^Z)

Inclusive Z/γ^* production and decay at hadron colliders

- Well known cross section
- Calculated up to NNLO



Motivations of p_T^Z measurements

- Provide a test of pQCD.
- Study the low p_T^Z region where non-perturbative effects may play a role.
 - Help in improving the modelling of W boson production needed for a precise measurement of the W mass.
 - Help in understanding the low p_T spectrum of the Higgs boson.

Latest p_T^Z measurements at the LHC: CMS Collaboration

Physics Letters B 749 (2015) 187-209: permil uncertainties at low p_T^Z

Table 1
Measured double differential fiducial cross section normalised to the inclusive fiducial cross section in units of GeV^{-1} .

q_T [GeV]	$0 \leq y < 0.4$			$0.4 \leq y < 0.8$			$0.8 \leq y < 1.2$			$1.2 \leq y < 1.6$			$1.6 \leq y < 2$		
	$\overline{d^2\sigma}/\sigma_{\text{inc}}$	δ_{stat} [%]	δ_{syst} [%]												
[0, 20]	2.10×10^{-2}	0.09	0.30	2.10×10^{-2}	0.09	0.30	1.96×10^{-2}	0.10	0.30	1.47×10^{-2}	0.12	0.31	7.88×10^{-3}	0.17	0.45
[20, 40]	6.20×10^{-3}	0.18	0.44	6.08×10^{-3}	0.19	0.42	5.50×10^{-3}	0.20	0.46	4.11×10^{-3}	0.24	0.59	2.17×10^{-3}	0.34	0.81
[40, 60]	2.28×10^{-3}	0.30	0.84	2.22×10^{-3}	0.31	0.80	1.99×10^{-3}	0.35	0.85	1.53×10^{-3}	0.40	1.03	8.11×10^{-4}	0.57	1.35
[60, 80]	9.79×10^{-4}	0.47	0.99	9.48×10^{-4}	0.48	0.94	8.85×10^{-4}	0.52	0.96	6.82×10^{-4}	0.62	1.16	3.75×10^{-4}	0.87	1.56
[80, 100]	4.73×10^{-4}	0.69	1.33	4.56×10^{-4}	0.71	1.26	4.23×10^{-4}	0.77	1.26	3.42×10^{-4}	0.89	1.43	1.92×10^{-4}	1.25	1.89
[100, 120]	2.33×10^{-4}	1.02	1.44	2.34×10^{-4}	1.01	1.36	2.19×10^{-4}	1.10	1.37	1.80×10^{-4}	1.25	1.50	1.01×10^{-4}	1.76	2.03
[120, 140]	1.31×10^{-4}	1.37	1.51	1.24×10^{-4}	1.42	1.50	1.15×10^{-4}	1.55	1.53	1.01×10^{-4}	1.72	1.58	6.03×10^{-5}	2.40	2.13
[140, 170]	6.42×10^{-5}	1.57	1.59	6.34×10^{-5}	1.57	1.54	6.05×10^{-5}	1.68	1.56	5.13×10^{-5}	1.93	1.68	3.00×10^{-5}	2.67	2.30
[170, 200]	2.88×10^{-5}	2.36	1.91	2.93×10^{-5}	2.35	1.88	2.90×10^{-5}	2.61	1.93	2.40×10^{-5}	2.98	2.14	1.49×10^{-5}	4.00	2.88
[200, 1000]	1.31×10^{-6}	2.01	1.64	1.30×10^{-6}	1.96	1.57	1.17×10^{-6}	2.21	1.75	9.90×10^{-7}	2.45	1.95	5.54×10^{-7}	3.39	2.39

Latest p_T^Z measurements at the LHC: ATLAS Collaboration

Eur. Phys. J. C (2016) 76:291: permit uncertainties at low p_T^Z

Table 30 The values of $(1/\sigma) d\sigma/dp_T^{Z\ell\ell}$ in each bin of $p_T^{Z\ell\ell}$ for the electron and muon channels separately (for various generator-level definitions) and for the Born-level combination in the kinematic region $66 \text{ GeV} \leq m_{\ell\ell} < 116 \text{ GeV}$, $0.0 \leq |y_{\ell\ell}| < 2.4$. The associated statistical and systematic (both uncorrelated and correlated between bins) are provided in percentage form

Bin	$(1/\sigma) d\sigma/dp_T^{Z\ell\ell} \pm \text{Statistical} [\%] \pm \text{Uncorrelated systematic} [\%] \pm \text{Correlated systematic} [\%]$					
	Electron channel		Muon channel		Combination	
	Dressed	Born	Bare	Dressed	Born	Born
0.0–2.0	2.608e-02 ± 0.3 ± 0.1 ± 0.9	2.677e-02 ± 0.3 ± 0.1 ± 0.9	2.568e-02 ± 0.2 ± 0.1 ± 0.9	2.626e-02 ± 0.2 ± 0.1 ± 0.9	2.696e-02 ± 0.2 ± 0.1 ± 0.9	2.669e-02 ± 0.2 ± 0.1 ± 0.5
2.0–4.0	5.441e-02 ± 0.2 ± 0.1 ± 0.5	5.553e-02 ± 0.2 ± 0.1 ± 0.6	5.337e-02 ± 0.1 ± 0.1 ± 0.3	5.428e-02 ± 0.1 ± 0.1 ± 0.3	5.541e-02 ± 0.2 ± 0.1 ± 0.4	5.545e-02 ± 0.1 ± 0.1 ± 0.2
4.0–6.0	5.505e-02 ± 0.2 ± 0.1 ± 0.3	5.560e-02 ± 0.2 ± 0.1 ± 0.3	5.483e-02 ± 0.1 ± 0.1 ± 0.4	5.525e-02 ± 0.1 ± 0.1 ± 0.4	5.579e-02 ± 0.1 ± 0.1 ± 0.5	5.590e-02 ± 0.1 ± 0.1 ± 0.3
6.0–8.0	4.831e-02 ± 0.2 ± 0.1 ± 0.4	4.831e-02 ± 0.2 ± 0.1 ± 0.5	4.856e-02 ± 0.2 ± 0.1 ± 0.2	4.851e-02 ± 0.2 ± 0.1 ± 0.2	4.851e-02 ± 0.2 ± 0.1 ± 0.6	4.847e-02 ± 0.1 ± 0.1 ± 0.3
8.0–10.0	4.084e-02 ± 0.2 ± 0.1 ± 0.4	4.052e-02 ± 0.2 ± 0.1 ± 0.5	4.115e-02 ± 0.2 ± 0.1 ± 0.2	4.085e-02 ± 0.2 ± 0.1 ± 0.2	4.055e-02 ± 0.2 ± 0.1 ± 0.6	4.047e-02 ± 0.1 ± 0.1 ± 0.3
10.0–12.0	3.429e-02 ± 0.2 ± 0.1 ± 0.2	3.389e-02 ± 0.2 ± 0.1 ± 0.3	3.458e-02 ± 0.2 ± 0.1 ± 0.2	3.420e-02 ± 0.2 ± 0.1 ± 0.2	3.378e-02 ± 0.2 ± 0.1 ± 0.4	3.384e-02 ± 0.1 ± 0.1 ± 0.2
12.0–14.0	2.881e-02 ± 0.2 ± 0.1 ± 0.3	2.838e-02 ± 0.2 ± 0.1 ± 0.3	2.919e-02 ± 0.2 ± 0.1 ± 0.2	2.878e-02 ± 0.2 ± 0.1 ± 0.2	2.835e-02 ± 0.2 ± 0.1 ± 0.3	2.838e-02 ± 0.2 ± 0.1 ± 0.2
14.0–16.0	2.431e-02 ± 0.3 ± 0.1 ± 0.3	2.393e-02 ± 0.3 ± 0.1 ± 0.3	2.479e-02 ± 0.2 ± 0.1 ± 0.2	2.443e-02 ± 0.2 ± 0.1 ± 0.2	2.403e-02 ± 0.2 ± 0.1 ± 0.2	2.404e-02 ± 0.2 ± 0.1 ± 0.1
16.0–18.0	2.076e-02 ± 0.3 ± 0.1 ± 0.2	2.041e-02 ± 0.3 ± 0.1 ± 0.2	2.109e-02 ± 0.2 ± 0.1 ± 0.2	2.077e-02 ± 0.2 ± 0.1 ± 0.2	2.042e-02 ± 0.2 ± 0.1 ± 0.2	2.043e-02 ± 0.2 ± 0.1 ± 0.1
18.0–20.0	1.782e-02 ± 0.3 ± 0.2 ± 0.3	1.755e-02 ± 0.3 ± 0.2 ± 0.3	1.805e-02 ± 0.3 ± 0.1 ± 0.2	1.781e-02 ± 0.3 ± 0.1 ± 0.2	1.756e-02 ± 0.3 ± 0.1 ± 0.2	1.756e-02 ± 0.2 ± 0.1 ± 0.2
20.0–22.5	1.510e-02 ± 0.3 ± 0.1 ± 0.3	1.490e-02 ± 0.3 ± 0.1 ± 0.3	1.520e-02 ± 0.3 ± 0.1 ± 0.3	1.503e-02 ± 0.3 ± 0.1 ± 0.3	1.485e-02 ± 0.3 ± 0.1 ± 0.3	1.488e-02 ± 0.2 ± 0.1 ± 0.2
22.5–25.0	1.259e-02 ± 0.3 ± 0.2 ± 0.4	1.247e-02 ± 0.3 ± 0.2 ± 0.4	1.275e-02 ± 0.3 ± 0.1 ± 0.2	1.266e-02 ± 0.3 ± 0.1 ± 0.2	1.253e-02 ± 0.3 ± 0.1 ± 0.2	1.251e-02 ± 0.2 ± 0.1 ± 0.2
25.0–27.5	1.072e-02 ± 0.4 ± 0.2 ± 0.4	1.065e-02 ± 0.4 ± 0.2 ± 0.4	1.074e-02 ± 0.3 ± 0.1 ± 0.3	1.068e-02 ± 0.3 ± 0.1 ± 0.3	1.061e-02 ± 0.3 ± 0.1 ± 0.3	1.062e-02 ± 0.2 ± 0.1 ± 0.2
27.5–30.0	9.172e-03 ± 0.4 ± 0.2 ± 0.5	9.124e-03 ± 0.4 ± 0.2 ± 0.5	9.089e-03 ± 0.3 ± 0.1 ± 0.3	9.064e-03 ± 0.3 ± 0.1 ± 0.3	9.014e-03 ± 0.3 ± 0.1 ± 0.3	9.062e-03 ± 0.3 ± 0.1 ± 0.2

⇒ Looking for any tiny effects on these precise measurements such as effect of p_T^Z binning.

why binning effect?

- p_T^Z measurement presentation:
 - Results of p_T^Z measurements are presented in the form: $\frac{1}{\sigma} \cdot \frac{d\sigma}{dp_T^Z}$, where σ is measured cross section in chosen phase space.
 - The measured p_T^Z spectrum (with **chosen binning**) is corrected for detector and QED final state radiation (FSR) effects **using an unfolding technique** to the underlying “true” spectrum.
- Which binning should be chosen for the p_T^Z distribution with more than 80% of statistics at low p_T^Z (< 30 GeV)?
 - Binning choices with same bin width lead to high statistical uncertainty at high p_T^Z .
 - Bin width at low p_T^Z is limited by the detector resolution.

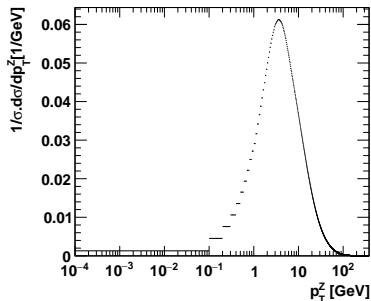
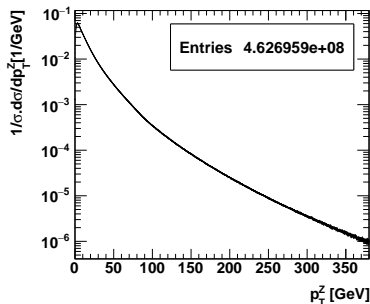
⇒ **Binning effect on these measurements needs to be quantified.**

What we do in this study?

- 1 Produce the “true” p_T^Z spectrum using a high statistical sample of one Monte-Carlo program (RESBOS).
- 2 Model the resolution of the p_T^Z measurement which presents the detector and QED final state radiation (FSR) effects.
- 3 Use several binning choices for the p_T^Z spectrum and smear the “true” p_T^Z spectrum with this resolution (folding procedure) to get the reconstructed p_T^Z spectrum and the response matrix for the unfolding procedure. (binning chosen with/without the requirement of purity of the reconstructed p_T^Z).
- 4 Unfold the reconstructed p_T^Z and then compare unfolded spectra with the “true” spectra in different cases of binning.

1. The “true” p_T^Z spectrum

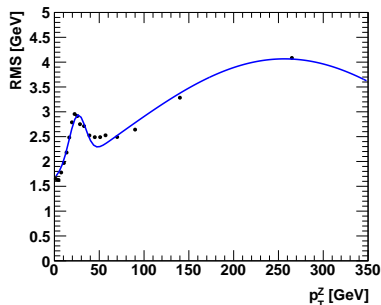
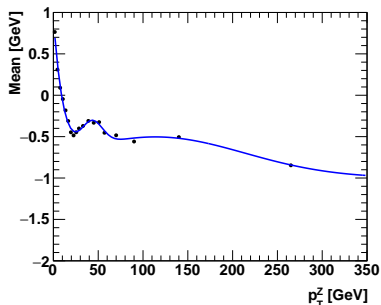
- In this study, the p_T^Z “true” spectrum (0 - 380 GeV) in proton-proton collisions at $\sqrt{s} = 7\text{TeV}$ is produced by the theoretical prediction program RESBOS which can describe data within 4% at low p_T^Z (JHEP09(2014)145, Eur. Phys. J. C (2016) 76:291).
- Selections: the lepton ($\ell = e, \mu$) transverse momentum $p_T^\ell > 20$ GeV, the lepton pseudorapidity $|\eta^\ell| < 2.4$ and the invariant mass of the lepton pair $66 \text{ GeV} < m_{\ell\ell} < 116 \text{ GeV}$.



2. Resolution of p_T^Z measurements

Resolution of p_T^Z measurements due to detector and QED FSR effects is modeled based on the information in [CERN-THESIS-2013-001](#) and is fitted by:

- The sum of 3 Gaussian functions for the mean of the resolution:
 $89.1077e^{-0.5[(x+88.143)/31.2624]^2} + 0.29835e^{-0.5[(x-42.8884)/11.7911]^2} + 0.496752e^{-0.5[(x-113.684)/99.9182]^2} - 1$
- The sum of 2 Gaussian functions for the rms of the resolution:
 $0.972987e^{-0.5[(x-25.5911)/9.27524]^2} + 4.06601e^{-0.5[(x-256.691)/191.119]^2}$



The “true” p_T^Z spectrum is then smeared by these resolution functions to obtain the reconstructed spectrum.

(Note that this resolution was of the p_T^Z measurements at the beginning of the ATLAS data taking in Run 1 and was higher than the resolution reached by the ATLAS now).

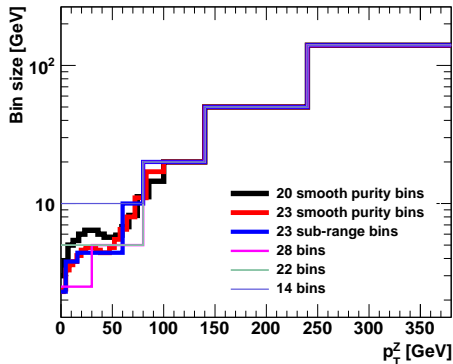
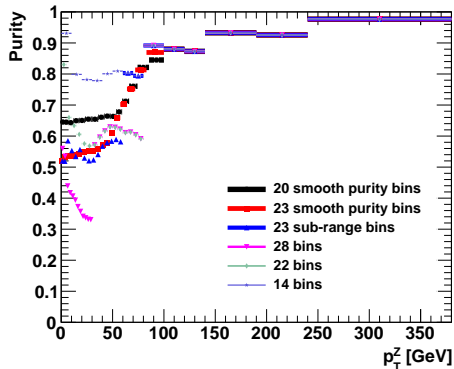
3. Purity, binning and smearing (1/4)

- Purity is the fraction of events reconstructed in a particular p_T^Z bin which have true p_T^Z in the same bin.
⇒ Relating to the event migration, higher purity corresponds with lower migration → control the unfolding procedure.

$$\text{Purity} = \frac{N_{\text{reconstructed and true events in the same bin}}}{N_{\text{reconstructed events in the bin}}}$$

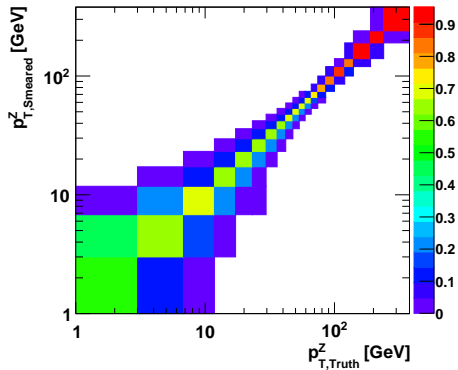
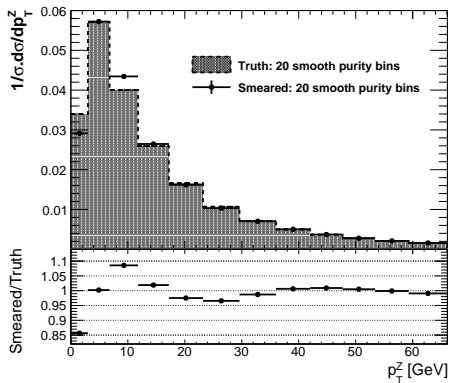
- Binning: 6 cases.
 - 20 bins with increasing purity ($> 65\%$).
 - 23 bins with increasing purity ($> 50\%$).
 - 23 bins with same bin sizes in sub-ranges.
 - 28 bins with 2.5 GeV bins at low p_T^Z .
 - 22 bins with 5 GeV bins at low p_T^Z .
 - 14 bins with 10 GeV bins at low p_T^Z .

3. Purity, binning and smearing (2/4)

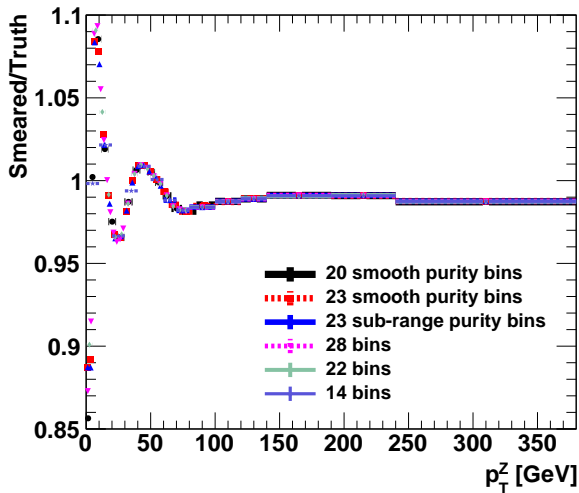


3. Purity, binning and smearing (3/4)

- Smearing:



3. Purity, binning and smearing (4/4)



Smearing effect is regular for all binning choices.

4. Unfolding the reconstructed p_T^Z spectra

- Instead of measuring \mathbf{x} one typically measures a related variable \mathbf{y} : $\mathbf{y} = \mathbf{A}\mathbf{x}$, \mathbf{A} is the response matrix describing detector effects
→ need an unfolding procedure to correct for detector effects and to obtain the true spectrum.
- Iterative Bayesian unfolding (implemented in RooUnfold package):

$$\hat{\mu}_i = \frac{1}{\epsilon_i} \sum_{j=1}^m p(t_i|o_j) n_j$$

$\hat{\mu}_i$: Number of events in truth

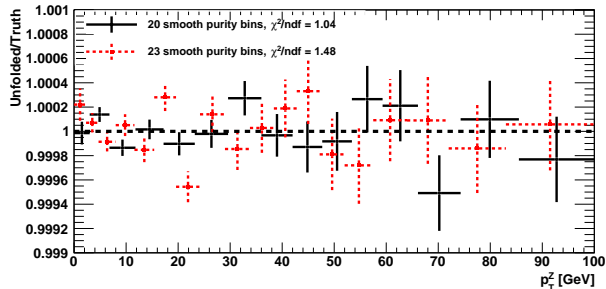
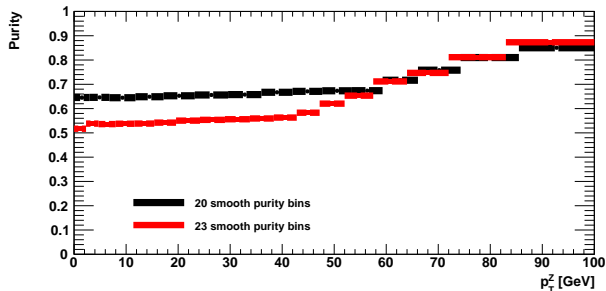
ϵ_i : Efficiency

$$p(t_i|o_j) = \frac{p(o_j|t_i)p_i}{\sum_{i=1}^N p(o_j|t_i)p_i}$$

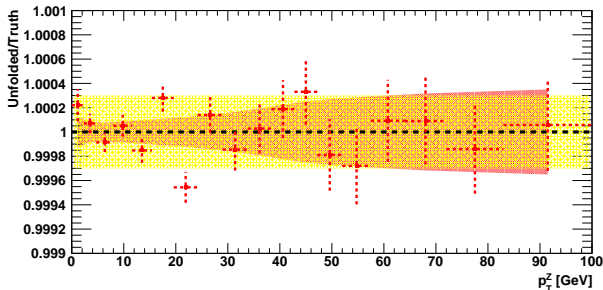
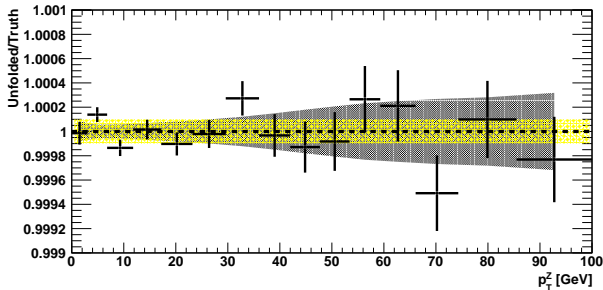
n_j : Number of events observed

$p(o_j|t_i)$ is the response matrix and can be inferred from Monte Carlo.

Results: 20 smooth purity bins vs 23 smooth purity bins

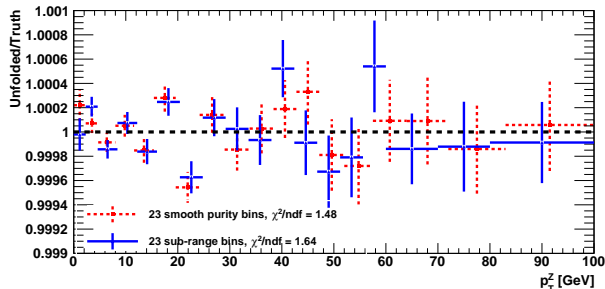
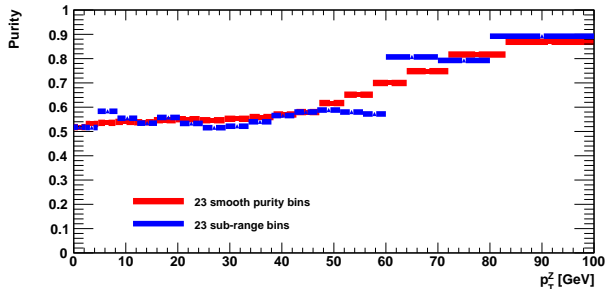


Results: 20 smooth purity bins vs 23 smooth purity bins



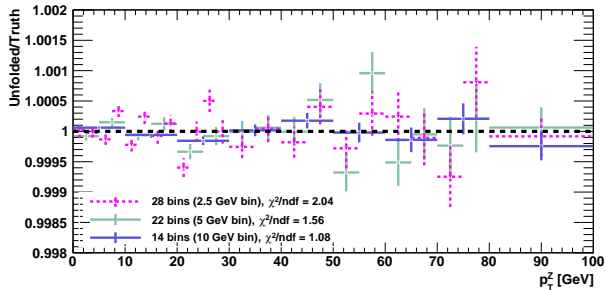
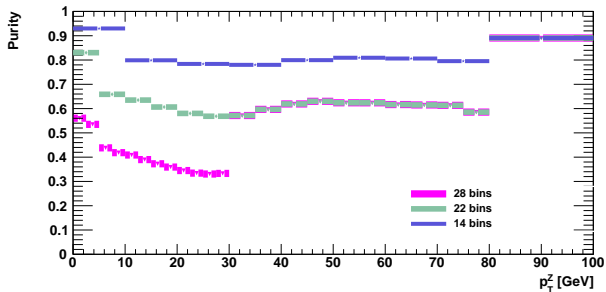
Reduce purity at low p_T^Z from 65% to 50% could increase binning effect to the level of 0.3‰ (yellow bands to show the order of effect)

Results: 23 smooth purity bins vs 23 sub-range purity bins

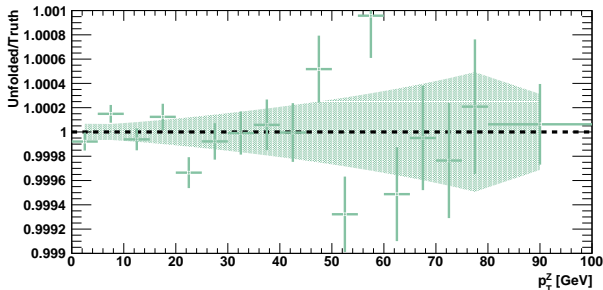
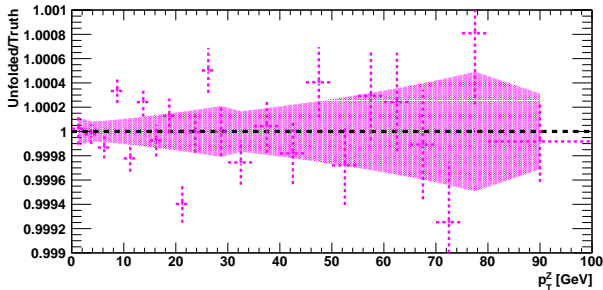


Different binning choices with purity in range of 50% – 65% at low p_T^Z would give the same effect.

Results: Same size binnings at low p_T^Z : 28 bins, 22 bins, 14 bins



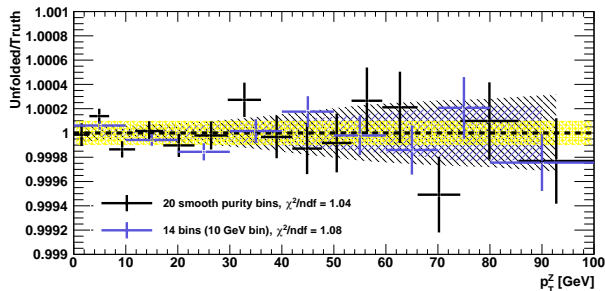
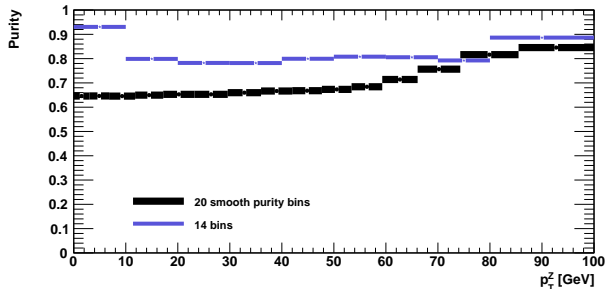
Results: Same size binnings at low p_T^Z : 28 bins, 22 bins, 14 bins



Same size binnings with purity below 65% at low p_T^Z would increase binning effect.

Binning optimization based on purity and statistics would give better results.

> 65% purity binning choices - stable results



Binning effect is negligible if purity of the p_T^Z measurement is increased as function p_T^Z from 65%.

- Reduce purity at low p_T^Z from 65% to 50% could increase binning effect to the level of 0.3 ‰.
- Different binning choices with purity in range 50% – 65% at low p_T^Z would give the same effect.
- Binning effect is negligible if purity of the p_T^Z measurement increases as function p_T^Z from 65%.

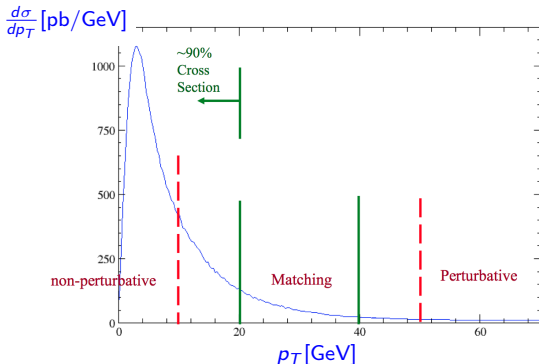
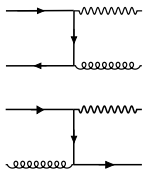
⇒ For the precise low p_T^Z measurements (permil uncertainties) with binning purity below 65%, 0.3‰ uncertainty due to the binning effect should be considered in the unfolding procedure.

Thank you for your attention!

Backup

p_T^Z predictions at hadron colliders

- At LO: $p_T^Z = 0$
- Beyond LO: $\frac{d\sigma}{dp_T^2}$ can be expressed in powers of α_s



For high $p_T^Z \rightarrow$ the contribution of higher orders in α_s decreases quickly
 \rightarrow a perturbative calculation is applicable.

- At NLO ($\mathcal{O}(\alpha_s)$), ($Q^2 = M_Z^2$):

$$\frac{d\sigma}{dp_T^2} = \alpha_s \left(A \frac{\ln(Q^2/p_T^2)}{p_T^2} + B \frac{1}{p_T^2} + C(p_T^2) \right),$$

where A and B are calculable coefficients and C is an integrable function.

p_T^Z predictions at hadron colliders at low p_T^Z

(Soft and collinear gluon emissions)

Dominant contributions to the differential cross section ($Q^2 = M_Z^2$):

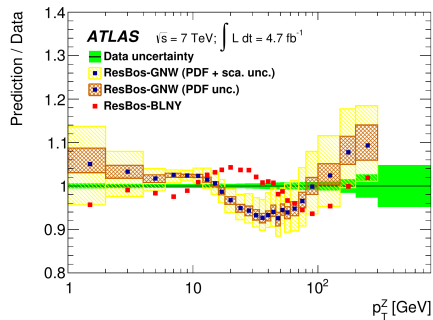
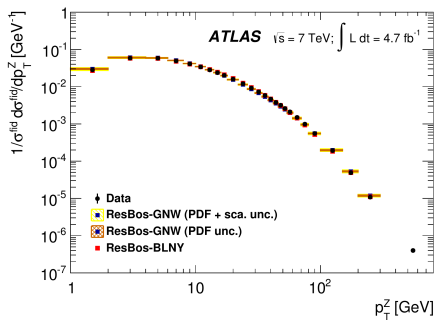
$$\frac{d\sigma}{dp_T^2} \sim \frac{\alpha_s}{p_T^2} \ln\left(\frac{Q^2}{p_T^2}\right) \left[v_1 + v_2 \alpha_s \ln^2\left(\frac{Q^2}{p_T^2}\right) + v_3 \alpha_s^2 \ln^4\left(\frac{Q^2}{p_T^2}\right) + \dots \right]$$

For $p_T \rightarrow 0$, $\alpha_s \ln^2(Q^2/p_T^2)$ is large even when α_s is small

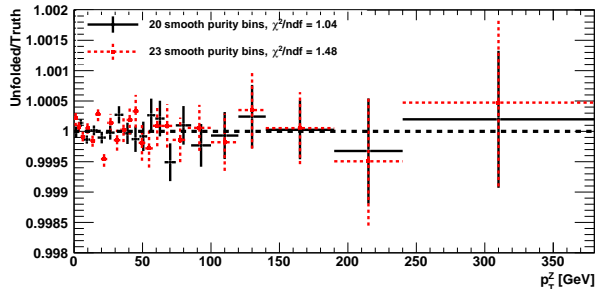
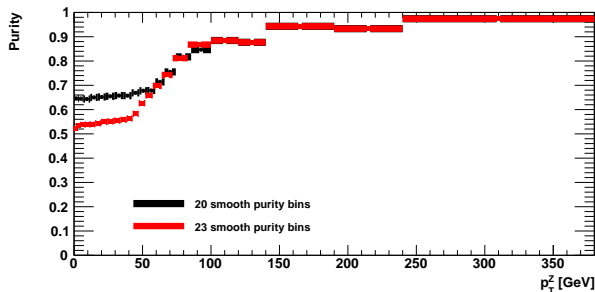
→ the p_T distribution diverges.

→ Two approaches:

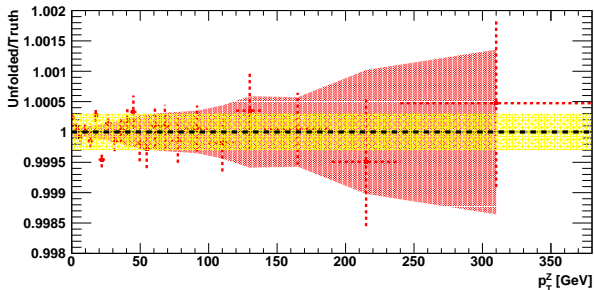
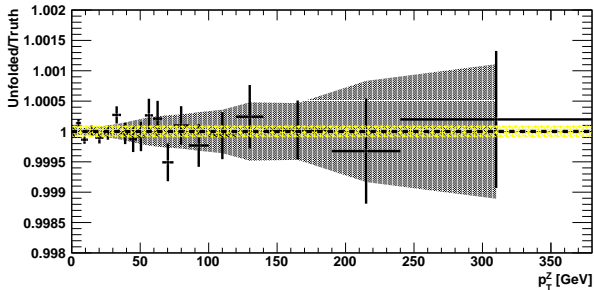
- Applying resummation of leading logarithms to all orders in α_s .
(RESBOS: Resummation + NLO corrected to $\mathcal{O}(\alpha_s^2)$ using K -factor)
- Or modeling by parton shower generators.



Results: 20 smooth purity bins vs 23 smooth purity bins

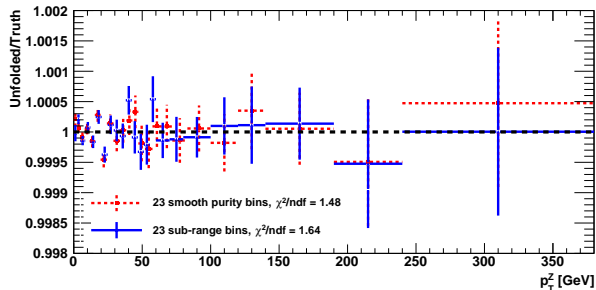
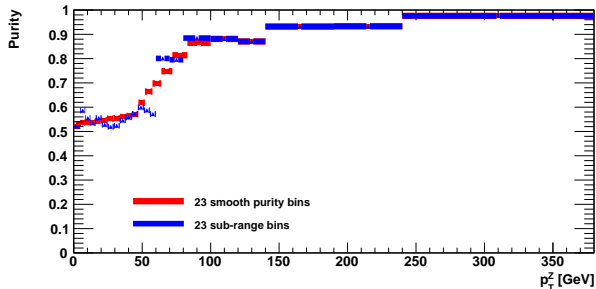


Results: 20 smooth purity bins vs 23 smooth purity bins



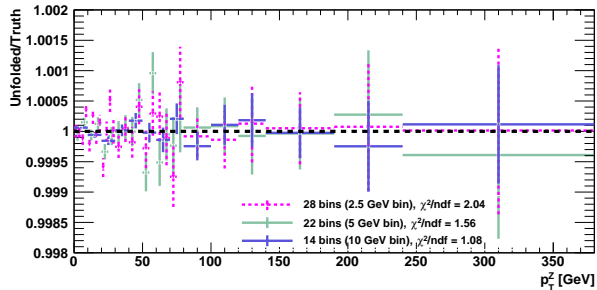
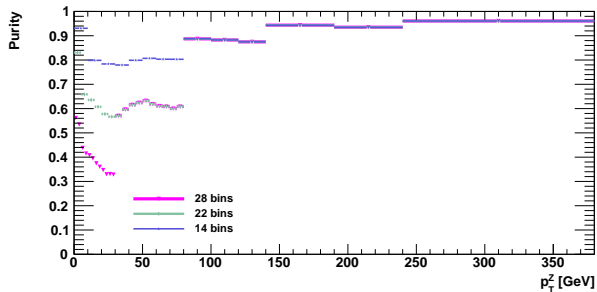
Reduce purity at low p_T^Z from 65% to 50% could increase binning effect to the level of 0.3‰ (yellow bands to show the order of effect)

Results: 23 smooth purity bins vs 23 sub-range purity bins

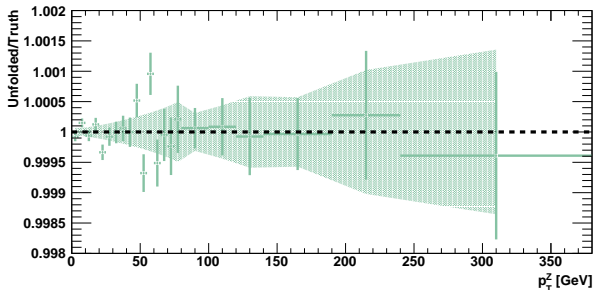
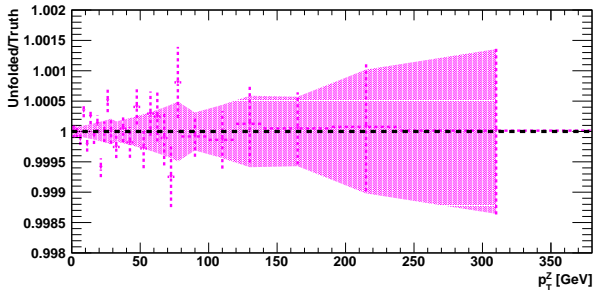


Different binnings with purity in range of 50% – 65% at low p_T^Z would give the same effect.

Results: Same size binnings at low p_T^Z : 28 bins, 22 bins, 14 bins



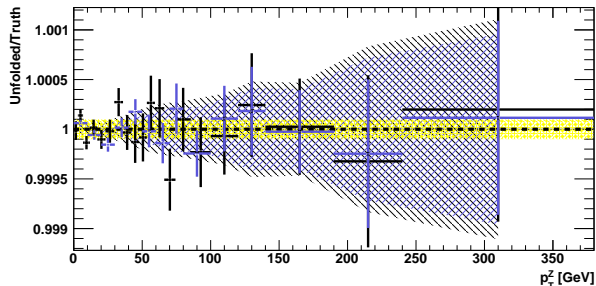
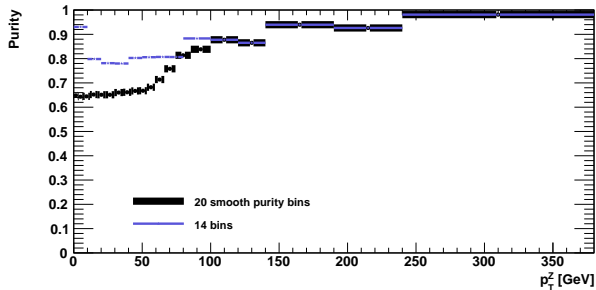
Results: Same size binnings at low p_T^Z : 28 bins, 22 bins, 14 bins



Same size binnings with purity below 65% at low p_T^Z would increase binning effect.

Binning optimization based on purity and statistics would give better results.

> 65% purity binning choice - stable results



Binning effect is negligible if purity of the p_T^Z measurement increases as function p_T^Z from 65%.